

Evaluation of Physical Properties of Pure Copper Fabricated by Electron Beam 3D Printer

Yohei Daino¹, Takashi Satoh¹, Kazuhiro Masuda¹, Shinichi Kitamura¹, Ippei Ohnuma²

¹3D Additive Manufacturing Project Development Group, JEOL Ltd., Akishima 196-8558, Japan

²Technical Development Department, NDK Inc., Sagamihara 252-0239, Japan

Abstract

Pure copper specimens were prepared using electron beam powder bed fusion (EB-PBF) to evaluate tensile strength, Vickers hardness, density, electrical conductivity, thermal conductivity and cracks caused by hydrogen embrittlement. Density was measured using the Archimedes method. Electrical conductivity was measured by an Eddy current conductivity meter. Thermal conductivity was measured by the laser flash method. Presence of cracks were evaluated by observing the cross section of the sample with Scanning Electron Microscope. As a result of the evaluation, the electrical conductivity was 101% IACS, the tensile strength was 203 MPa and the thermal conductivity was $380 \text{ W} \cdot \text{m}^{-1} \cdot \text{K}^{-1}$. These values are excellent for samples produced by a 3D printer. This suggests that higher quality pure copper parts can be obtained by using an electron beam as a heat source for the 3D printer.

Keywords: Additive Manufacturing, 3D Printer, Electron beam melting, Pure-Copper, Characterization, Tensile Test, Vickers hardness, density, Electrical conductivity, Thermal Conductivity, Crack

1. Introduction

There are various types of devices with different process in 3D printers. Typical methods are the powder bed fusion (PBF), direct energy deposition (DED) and binder jet (BJ) [1]. PBF process have two types: EB-PBF, which uses an electron beam as the heat source, and LB-PBF, which uses a laser beam.

This paper describes the fabrication of pure copper parts using the EB-PBF.

There are several advantages when pure copper parts are fabricated with EB-PBF compared to LB-PBF [2]. The LB-PBF uses a fiber laser as the light source and its wavelength is between 1030 and 1070 μm . However, Pure copper absorbs only approximately 2% of the light in that wavelength range, so most of the input energy cannot contribute to melting. On the other hand, the energy conversion efficiency of the electron beam impacting the material is approximately 80%. In other words, in the case of electron beams, the majority of the input energy contributes to melting without being affected by the emissivity of powder surface [3][4].

It has also been reported that for additive manufacturing of pure copper, fast beam scanning speeds are required to obtain crack-free parts with good electrical conductivity [5]. However, in the case of laser systems, high speed scanning is difficult due to mechanical scanning with galvanometric mirrors. On the other hand, in electron beam scanning, the beam is scanned by electromagnetic deflection as in scanning electron microscopes, so the beam can scan at high speed and high accuracy.

In short, EB-PBF allows higher energy input and faster beam scanning than LB-PBF, which could be advantageous in the fabrication of pure copper.

Pure copper parts made by additive manufacturing have the problem of cracking due to hydrogen embrittlement. [3].

Therefore, the aim of this paper is to fabricate pure copper

specimens using EB-PBF to evaluate hydrogen embrittlement cracking and to evaluate their mechanical and physical properties.

2. Experiment

2.1 Powder material

Experiments were carried out using copper powder with a purity of 99.9%. The powders used in the experiments are shown in Figure 1. The powder is prepared by disc atomization method, which has higher sphericity and better flowability than those prepared by gas atomization method. The respective properties of the powder are apparent density of $5.21 \text{ g} \cdot \text{cm}^{-3}$, flowability of $11.35 \text{ s} \cdot 50\text{g}^{-1}$, mean particle diameter of $72 \mu\text{m}$ and oxygen concentration of 200 wt.ppm.

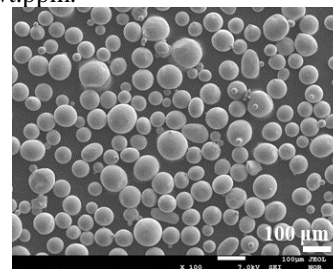


Figure 1. SEM image of Pure Copper Powder.

2.1 3D printer machine

The experiments were carried out using an in-house developed 3D printer. The specification of the developed machine is listed in Table 1. This machine is EB-PBF and the electron gun cathode is LaB₆. For comparison, the specifications of a typical LB-PBF machine are listed in Table 2. The sizes of the build envelope are comparable. The minimum beam spot size of the developed in-house EB-PBF machine is $180 \mu\text{m}$, while the laser machine's minimum beam size is $61 \mu\text{m}$. On the other hand, the beam scanning speed of the EB-PBF is $280 \text{ m} \cdot \text{s}^{-1}$, whereas for lasers it is $4.5 \text{ m} \cdot \text{s}^{-1}$. In addition, the laser power of the EB-PBF is 6 kW and that of the LB-PBF is 2kW. In short,

EB-PBF is slightly inferior to LB-PBF in terms of beam spot size, but has a much superior beam scanning speed and beam power.

Table 1. In-House Developed 3D Printer Machine

Process	EB-PBF
Max. Build Size	$\phi 260 \times 400$ mm(h)
Cathode Type	Lab ₆
Acceleration Voltage	60 /kV
Max. Beam Power	6 /kW
Min. Beam Diameter	180 / μ m
Max. Beam Scanning Speed	280 /m \cdot s ⁻¹

Table 2. Laser Powder Bed Fusion Machine [3]

Process	LB-PBF
Max. Build Size	245 \times 245 \times 400 mm(h)
Laser Type	Fiber Laser
Max. Laser Power	2 \times 1 /kW
Min. Beam Diameter	61 / μ m
Max. Beam Scanning Speed	4.5 /m \cdot s ⁻¹

2.2 Specimen fabrication

Photographs of objects fabricated by EB-PBF are shown in Figures 2 and 3. Oxygen free copper (OFC) with a diameter of 210 mm and a thickness of 20 mm was used for the starting plate. For the preparation of test specimens, rectangles (15 \times 100 \times 15 mm) and cubes (15 \times 15 \times 15 mm) were fabricated by EB-PBF. Test specimens for tensile tests, thermal conductivity measurements, Vickers hardness were cut from these objects. In addition, cubes (20 \times 20 \times 20 mm) were fabricated as samples for electrical conductivity and density measurements.

Examples of the preparation of each specimen are shown in Figures 4(a) to (c). (a) is for tensile test, (b) is for Archimedes density measurement and (c) is for Vickers hardness. The process parameters are listed in Table 3. The experiments were carried out at a process temperature of 550 $^{\circ}$ C to 600 $^{\circ}$ C. During melting, the scan speed is 4.5 m/s, the beam current is 20.0 mA and the beam diameter is 250 μ m. These are optimized parameter before this examination.

Table 3. Process parameters

Heating	Temperature / $^{\circ}$ C	550 - 600
Melting	Scan Speed /m \cdot s ⁻¹	4.50
	Beam Current /mA	20.0
	Beam Diameter / μ m	250

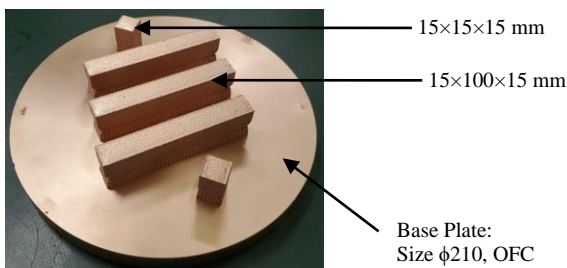


Figure 2. The Object Fabricated by In-House 3D Printer.

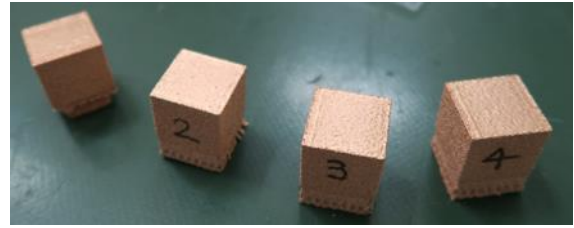


Figure 3. Specimens for Evaluation of Electric Conductivity.

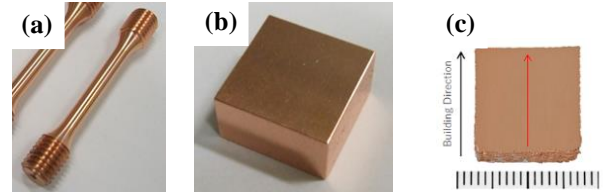


Figure 4. Specimens, (a)Specimen for tensile test, (b)Specimen for Archimedes method, (c)Specimen for Vickers hardness test.

3. Results

3.1 Mechanical Properties

Tensile and hardness tests and density measurement tests were carried out to evaluate the mechanical properties.

Tensile tests were performed according to ASTM E8/E8M-22 using the specimen shown in Figure 4(a). An INSTRON 5982 was used for the tests. The results showed an ultimate tensile strength of 203 MPa, a yield stress of 73 MPa, a Young's modulus of 92 GPa and an elongation of 57.3%.

As shown in Figure 4(c), cube samples were cut in half and Vickers hardness was measured at 1 mm intervals from bottom to top surface. The relationship between Vickers hardness and building height is shown in Figure 5. Vickers hardness does not change significantly with building height and was 53.3 HV0.05 at the center of the specimen.

Density measurements were performed using the Archimedes method with the cube object prepared as shown in Figure 4(b). The density was 8.92 g \cdot cm⁻³. Assuming a true density of 8.94 g \cdot cm⁻³, the relative density is 99.7 %.

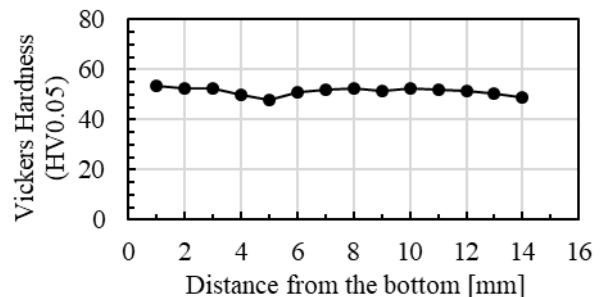


Figure 5. Relationship between Vickers hardness and Building Direction.

3.4 Electrical conductivity and Thermal conductivity

IACS conductivity evaluation was carried out using an eddy current conductivity meter. Measurements were taken

three times on each of the four samples and all results were 100% IACS or better. The thermal conductivity was evaluated by laser flash method. The sample size is $\phi 10 \times 2$ mm. $381 \text{ W} \cdot \text{m}^{-1} \cdot \text{k}^{-1}$ was obtained at a measurement temperature of $25 \text{ }^\circ\text{C}$.

3.5 Observation of cross section

Cross sections of cube samples were observed using scanning electron microscopy. The backscattered electron image and the binary image are shown in Figure 6. (a) is the sample obtained in this study. (b) is its binarized image. (c) is a sample with hydrogen embrittlement prepared as a reference. (d) is its binarized image. It is generally said that cracks occur when pure copper is fabricated by additive manufacturing, but this experiment fabricates samples with fewer cracks. In addition, the relative density by image analysis is 99.97 %, indicating that a high-density sample was obtained.

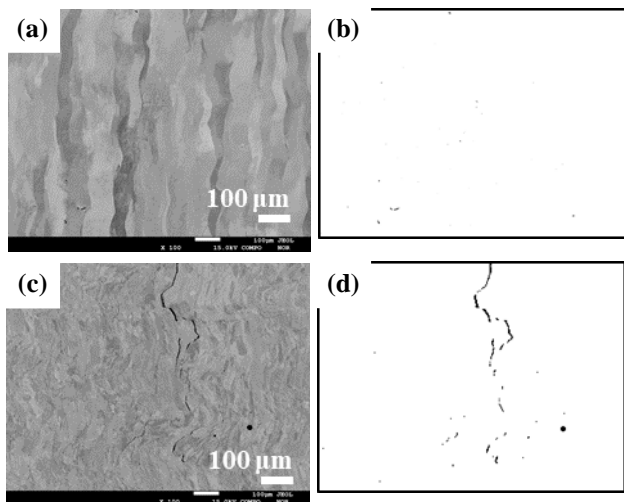


Figure 6. Cross section image of the sample observed by SEM. (a) Crack free sample, (b) Binary Image of crack free sample, (c) Binary Image of crack sample, (d) Binary Image of crack sample.

4. Discussion

The mechanical strength, thermal conductivity and electrical conductivity values of pure copper made from LB-PBF and EB-PBF from the previous literature are summarized in Table 4 together with the results of the present examination.

The best results for tensile strength are obtained with LB-PBF. This is due to the fact that EB-PBF is a hot process.

Tests conducted by Ralf Guschlbauer et al. in EB-PBF [5] reported that cracking due to hydrogen embrittlement is a problem. They predicted that the high oxygen concentration could have caused the cracking. In the tests we carried out this time, no cracking was observed. This is probably due to the different oxygen concentrations of the fabricated parts: in the tests conducted by Ralf Guschlbauer et al. the oxygen concentration of the sample parts was 200 wt.ppm, while in the tests conducted by Suraj Dinkar Jadhav et al. the oxygen concentration of the samples was 54 wt.ppm, and the oxygen concentration of our sample parts was 14

wt.ppm. In addition, Ralf Guschlbauer et al. reported cracks in their samples and Suraj Dinkar Jadhav et al. did not specifically mention cracks. This means that our sample is not cracking due to particularly low oxygen concentrations.

Table 4. Comparison with previous literature

	This Study (EB-PBF)	LB-PBF [4]	EB-PBF [5]
Tensile Strength /MPa	203	211	177
Yield stress /MPa	73	122	78
Elongation /%	57.3	43	59.3
Density / $\text{g} \cdot \text{cm}^{-3}$	8.92	8.88 ^{※1}	8.84
Thermal conductivity / $\text{W} \cdot \text{m}^{-1} \cdot \text{k}^{-1}$	381	392	411.9
Electrical Conductivity /%IACS	101	94	> 100

※1: Calculated values from the values in the paper. In Paper [4], only relative densities were given.

5. Conclusions

Pure copper parts were fabricated by EB-PBF. Better values were obtained for mechanical strength, thermal conductivity and electrical conductivity. Cracking due to hydrogen embrittlement was also prevented. These showed that EB-PBF could be effective in forming of pure copper.

Since excellent physical properties were obtained with simple geometries, it is necessary to investigate whether better results can be obtained with more complex geometries in the future.

References

- 1) W. J. Sames and F. A. List, S. Pannala, R. R. Dehoff, S. S. Babu: *International Materials Reviews*. **61** (2016) 315-360
- 2) Carolin Körner: *International Materials Reviews*. **61** (2016) 361-377
- 3) Ralf Guschlbauer and Alex K. Burkhardt, Zongwen Fu, Carolin Körner: *Materials Science & Engineering A*. **779** (2020) 139106.
- 4) Suraj Dinkar Jadhav and Louca Raphaël Goossens, Yannis Kinds, Brecht Van Hooreweder, Kim Vanmeensel: *Additive Manufacturing*. **42** (2021) 101990.
- 5) Ralf Guschlbauer and Soroush Momeni, Fuad Osmanlic, Carolin Körner: *Materials Characterization*. **143** (2018) 163-170.
- 6) GE Additive, Concept Laser M2 Series 5, https://www.ge.com/additive/sites/default/files/2023-08/DMLM_M2Series5_Bro_4_A4_EN_3.pdf. (Accessed 20 August 2023)